

Supplementary Information

Hydropower plans in eastern and southern Africa increase risk of concurrent climate related electricity supply disruption

Declan Conway^{1,*}, Carole Dalin^{1,2}, Willem A. Landman³, Timothy J. Osborn⁴

Affiliations:

¹ Grantham Research Institute on Climate Change and the Environment, London School of Economics and Political Science, Houghton Street, London, UK;

² Institute for Sustainable Resources, Bartlett School of Environment, Energy and Resources, University College London, London, UK.

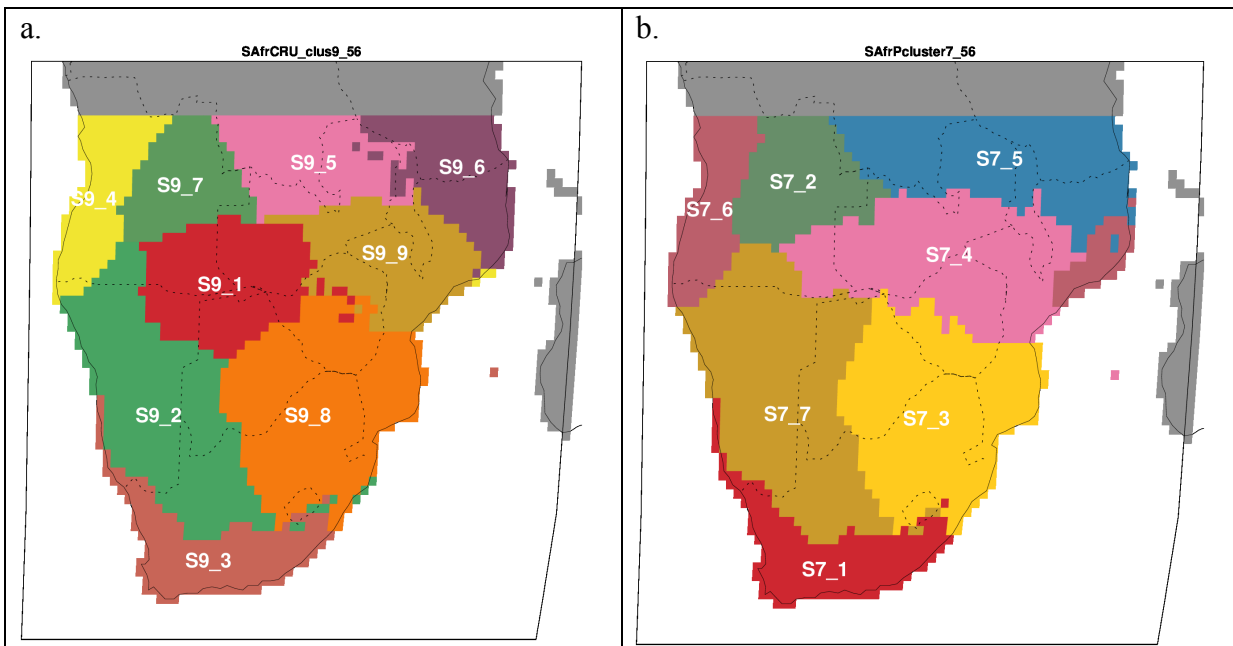
³ Department of Geography, Geo-informatics and Meteorology, University of Pretoria, Pretoria, South Africa;

⁴ Climatic Research Unit, School of Environmental Sciences, University of East Anglia, Norwich Research Park, Norwich, UK;

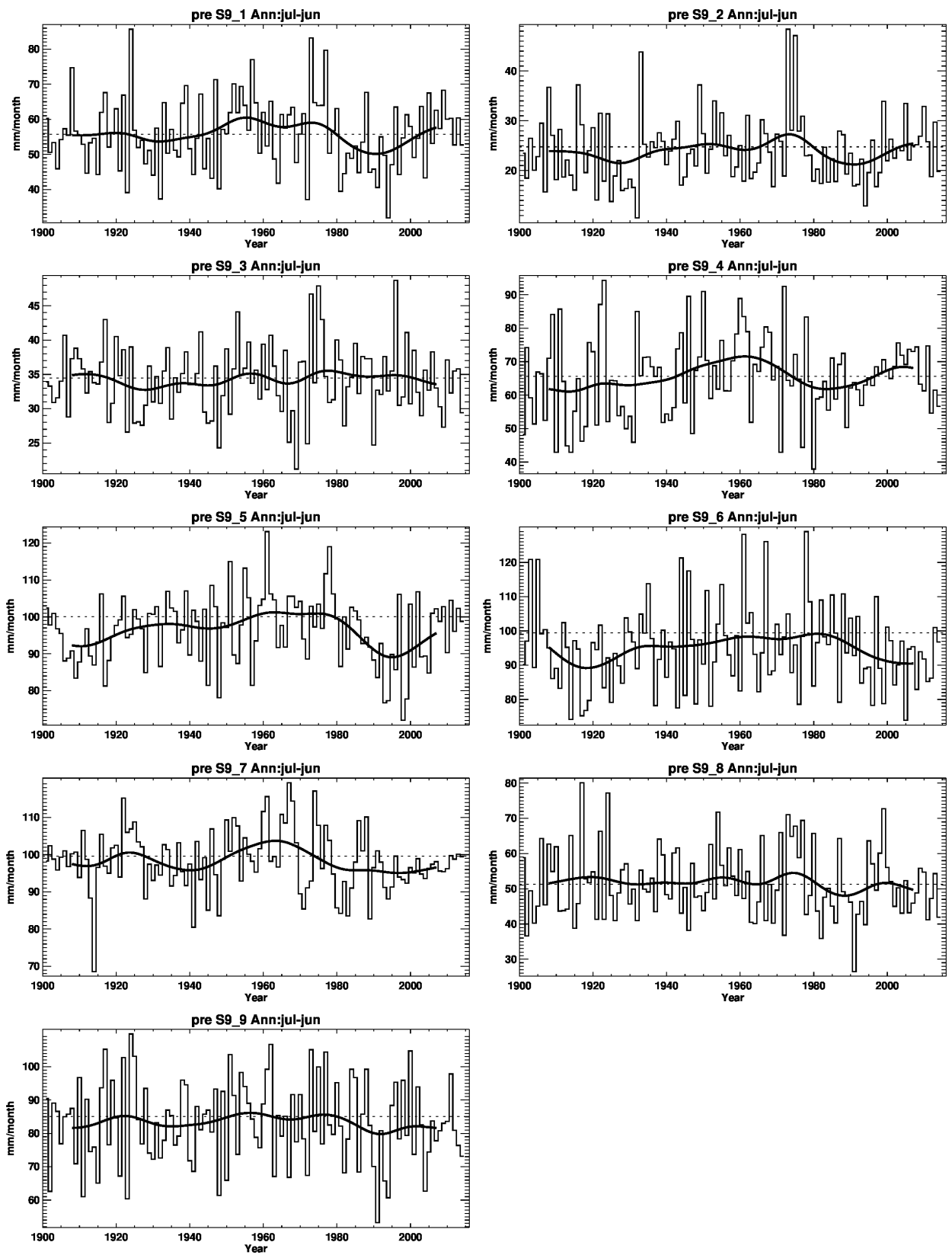
*Correspondence to: d.conway@lse.ac.uk

Content

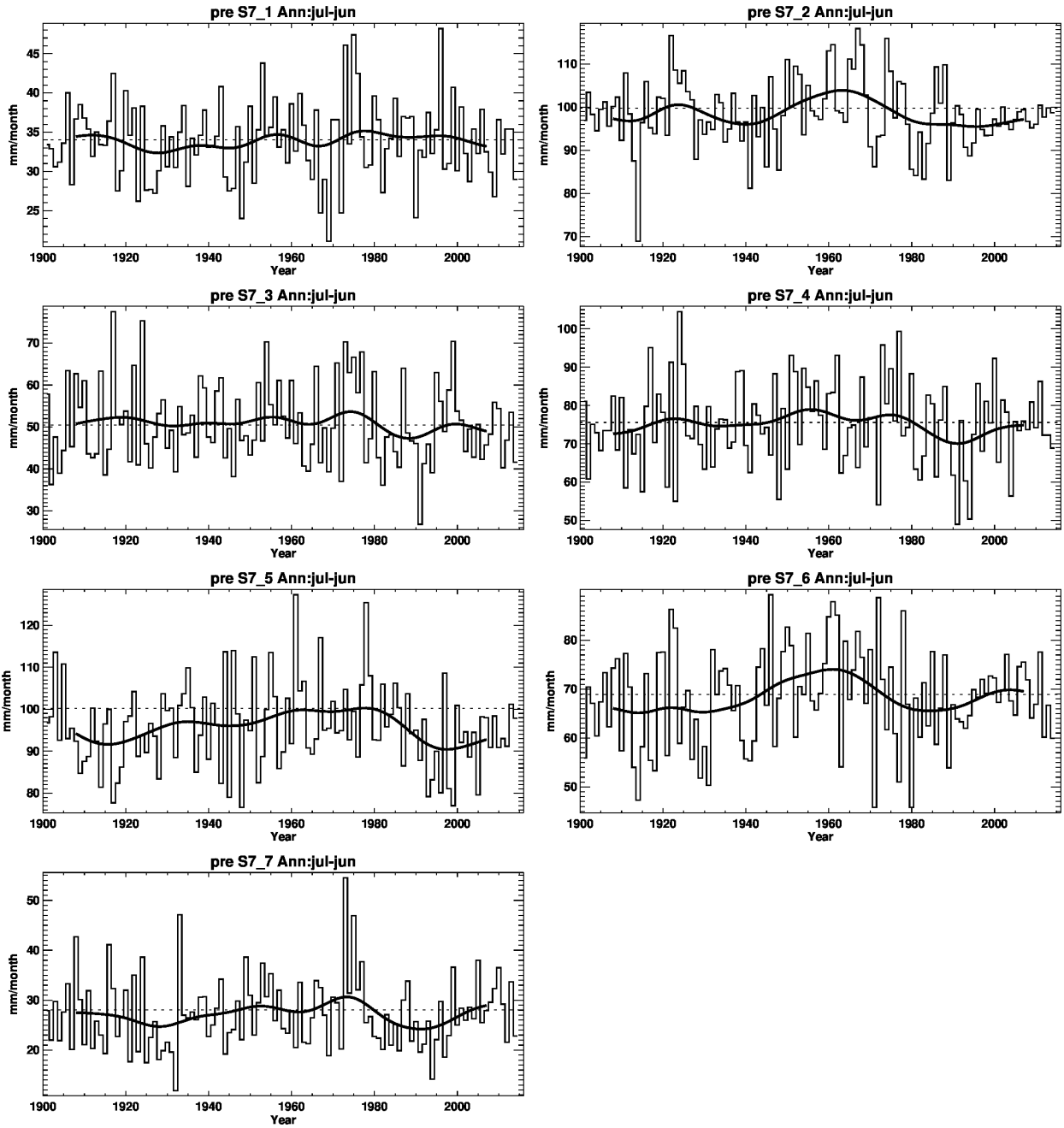
Supplementary Figures 1-12	2
Supplementary Tables 1-18	11
Supplementary Notes 1-6	25
Supplementary Note 1: Southern Africa full results; 1956/57-2010/11	25
Supplementary Note 2: Eastern Africa full results; 1956-2011	28
Supplementary Note 3: Temporal stability of clusters and correlations	29
Supplementary Note 4: Central Africa and the Grand Inga dam	30
Supplementary Note 5: Variance explained by principal components	30
Supplementary Note 6: Collection and categorization of existing and proposed hydropower sites in Eastern and Southern Africa	31
Supplementary References	32



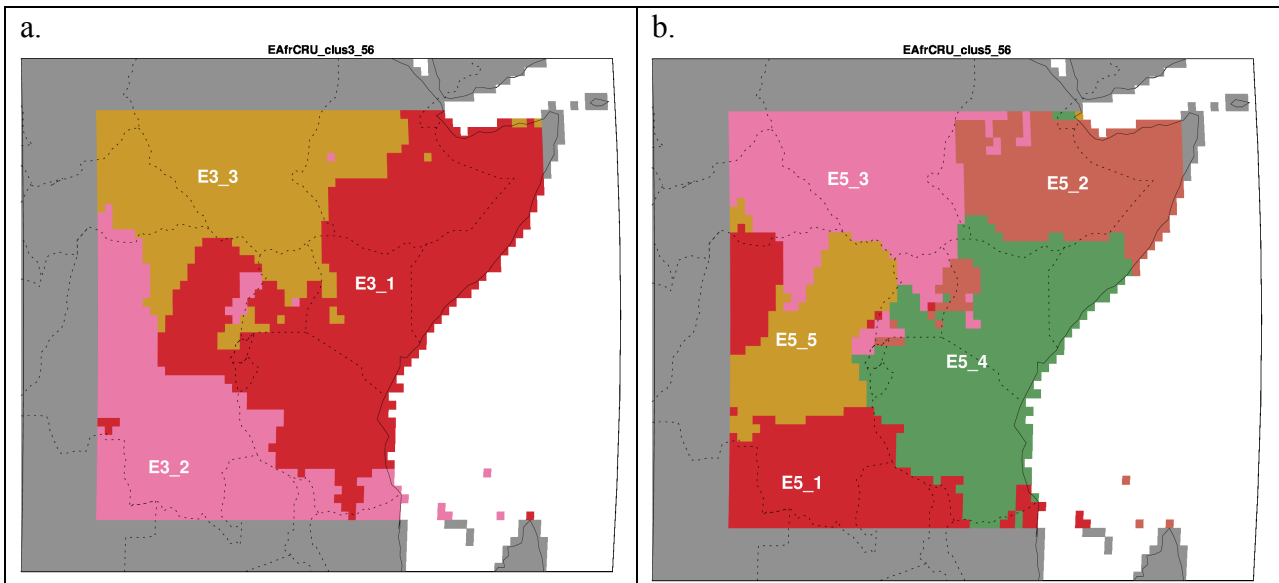
Supplementary Figure 1. Spatial definitions for nine (a.) and seven (b.) clusters in southern Africa (1956/57-2010/11). See labelling for cluster number.



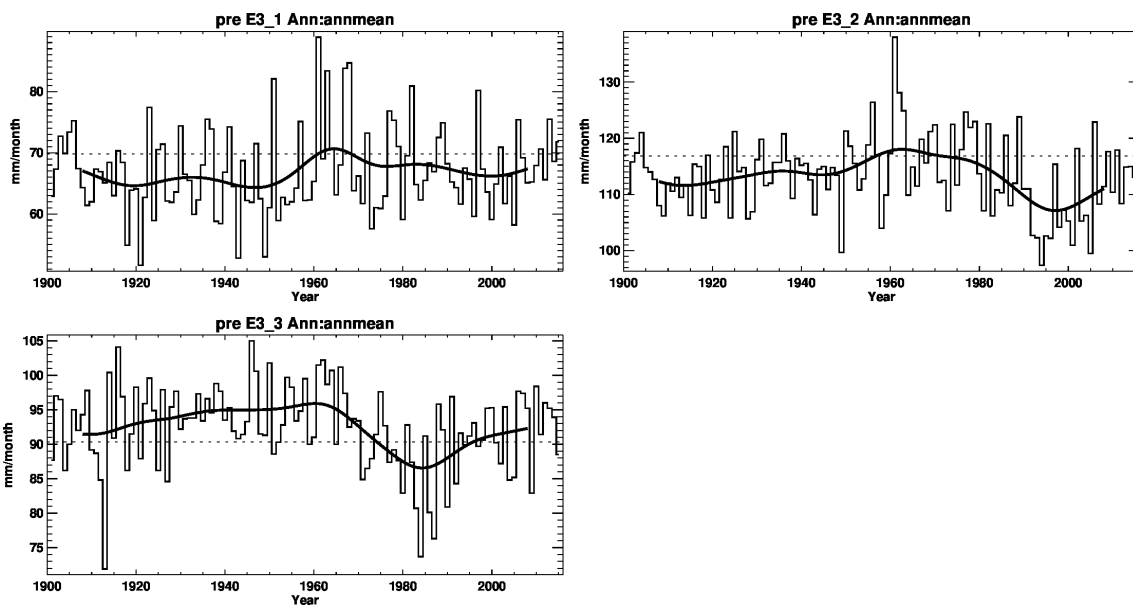
Supplementary Figure 2. Annual-mean (July to June) cluster-mean precipitation (mm/month) from CRU TS3.24 (1, updated) for the 9 clusters, for 1901/2 to 2014/5. Thin lines show individual yearly values (aligned with the year in which the average begins – i.e. the 2000 value is July 2000 to June 2001); thick line shows 30-year smoothed; horizontal dashed line shows 1961-1990 climatological mean.



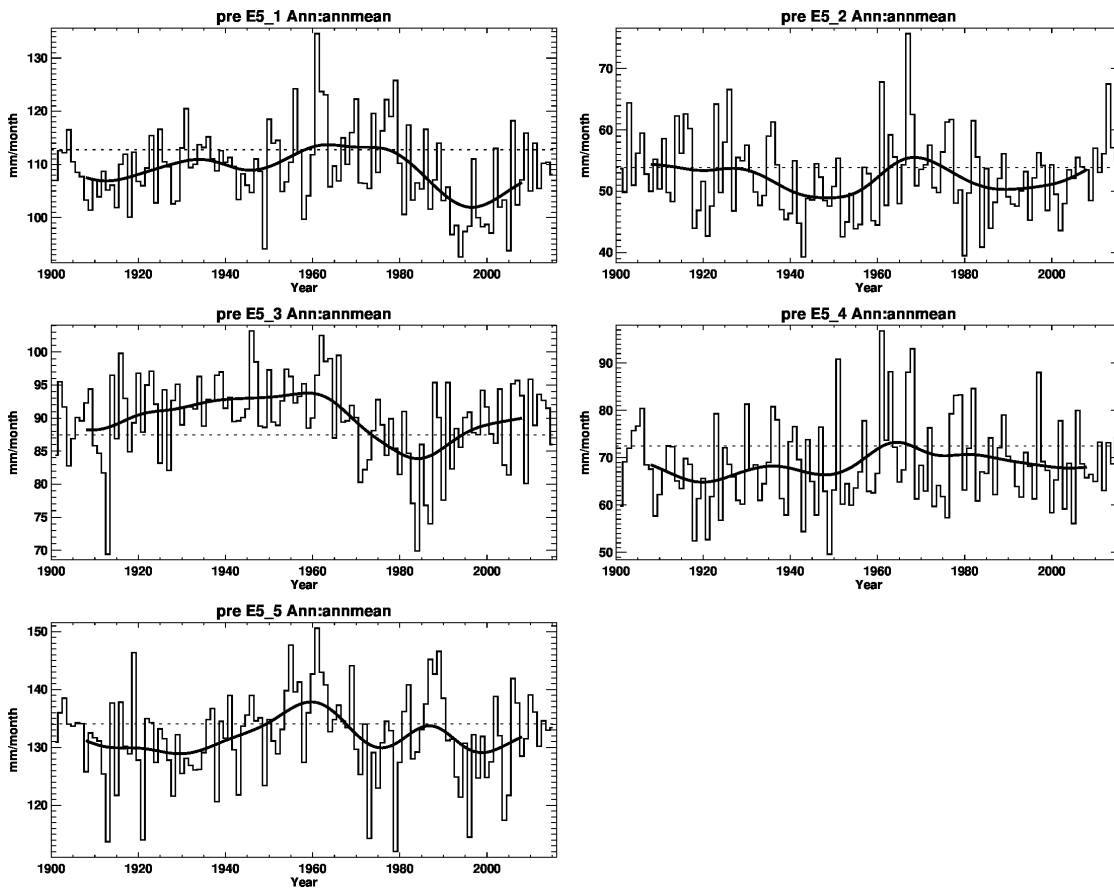
Supplementary Figure 3. As Supplementary Figure 3 but for 7 clusters.



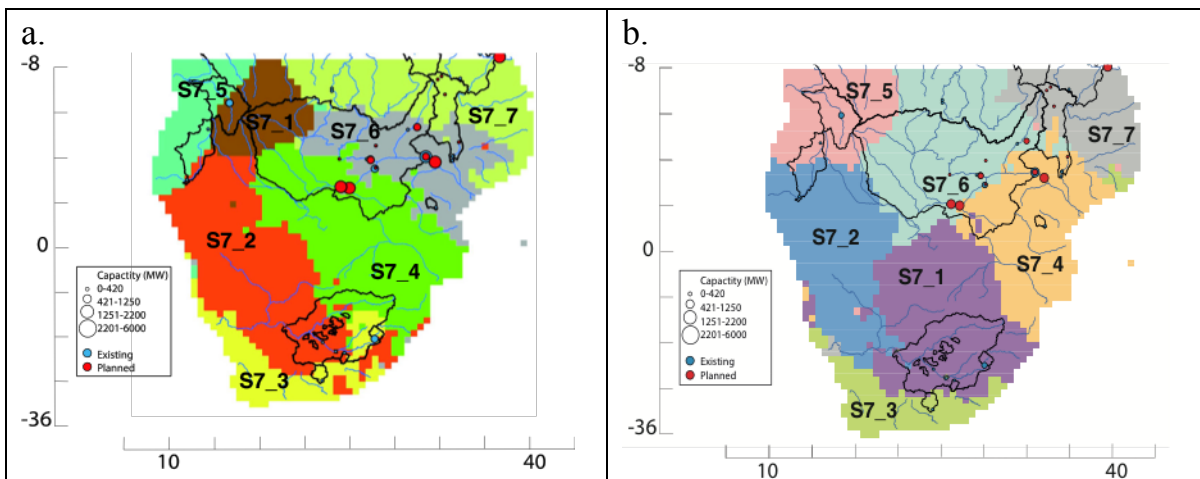
Supplementary Figure 4. Spatial definitions for three (a) and five (b) clusters in eastern Africa (1956-2011). See labelling for cluster number.



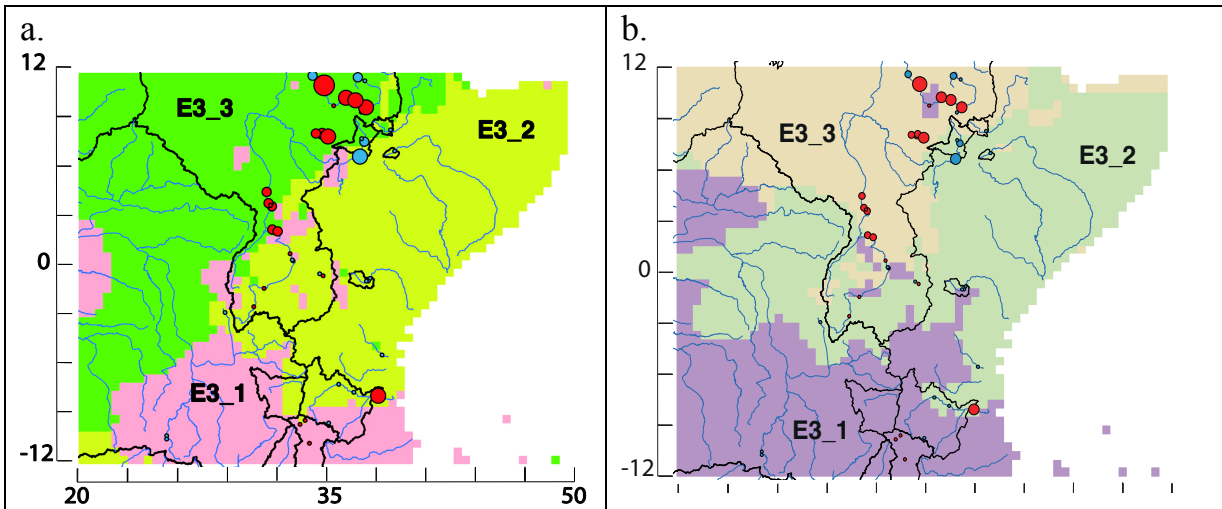
Supplementary Figure 5. Annual-mean (January to December) regional-mean precipitation (mm/month) from CRU TS3.23 (1, updated) for the 3 clusters, for 1901 to 2014. Thin lines show individual yearly values; thick line shows 30-year smoothed; horizontal dashed line shows 1961-1990 climatological mean.



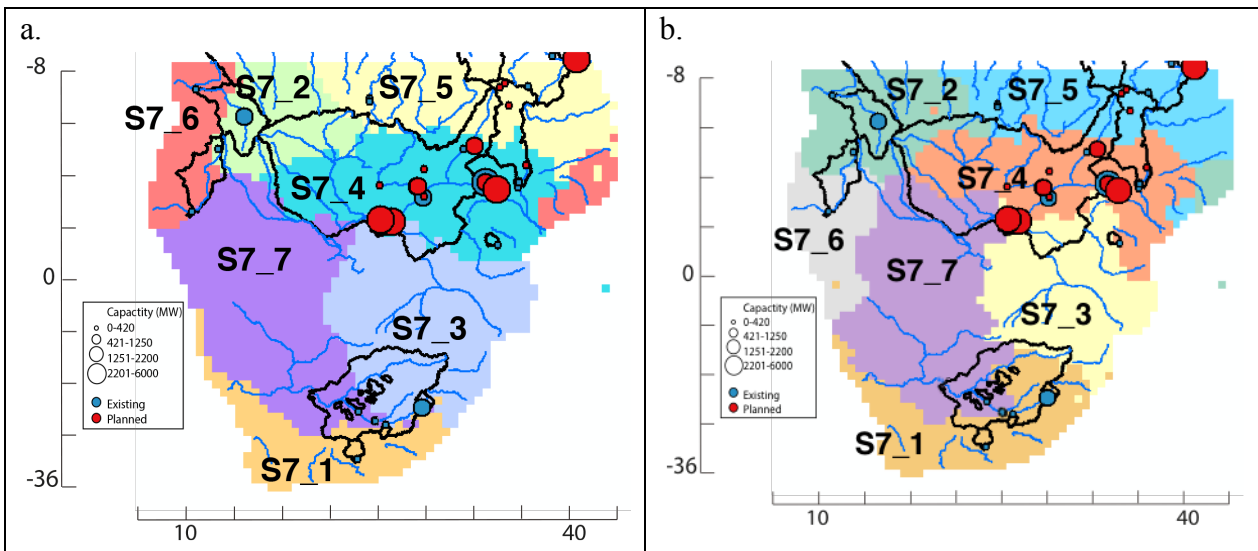
Supplementary Figure 6. As Supplementary Figure 7 but for 5 clusters.



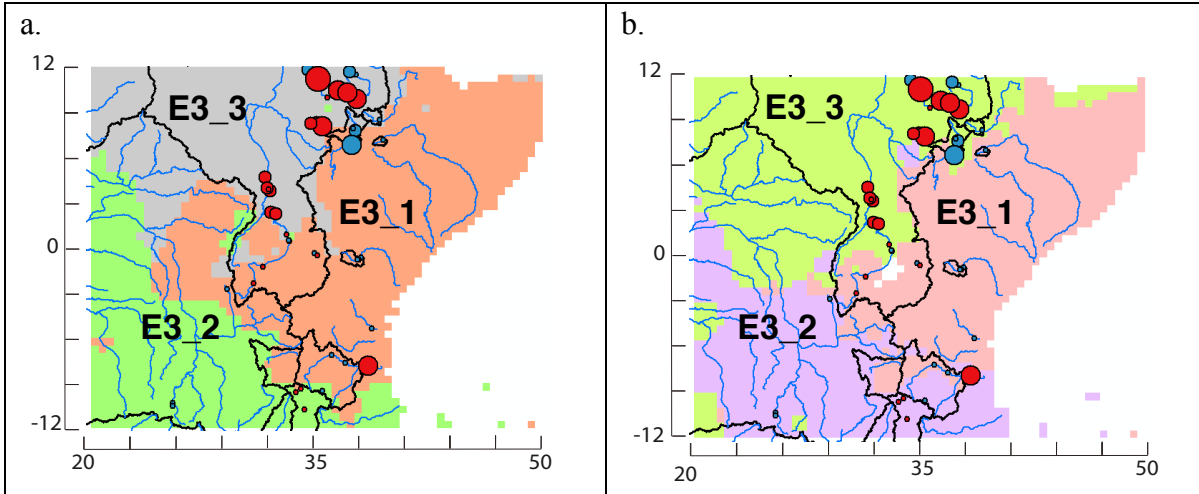
Supplementary Figure 7. Map of seven clusters and main river basin outlines for southern Africa, (a.) results for 1951-1980, (b.) results 1981-2011. Note the full basin outline shown for the Orange River was not used for calculations and three Pumped Storage Schemes (small basins adjacent to Orange basin) were also not used (See Supplementary Table 17 for list of dams used).



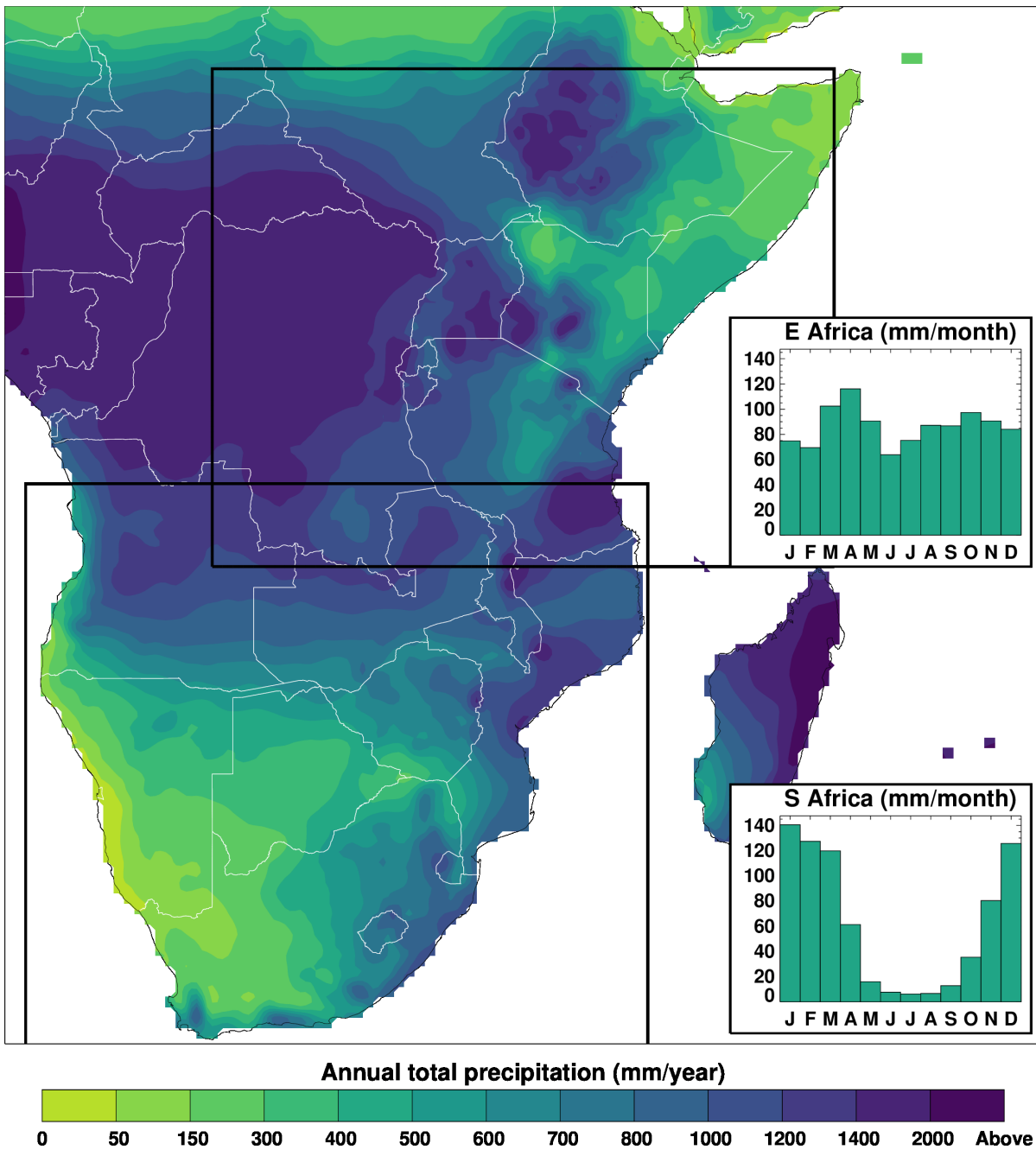
Supplementary Figure 8. Map of three clusters and main river basin outlines for eastern Africa, (a.) results for 1951-1980, (b.) results 1981-2011.



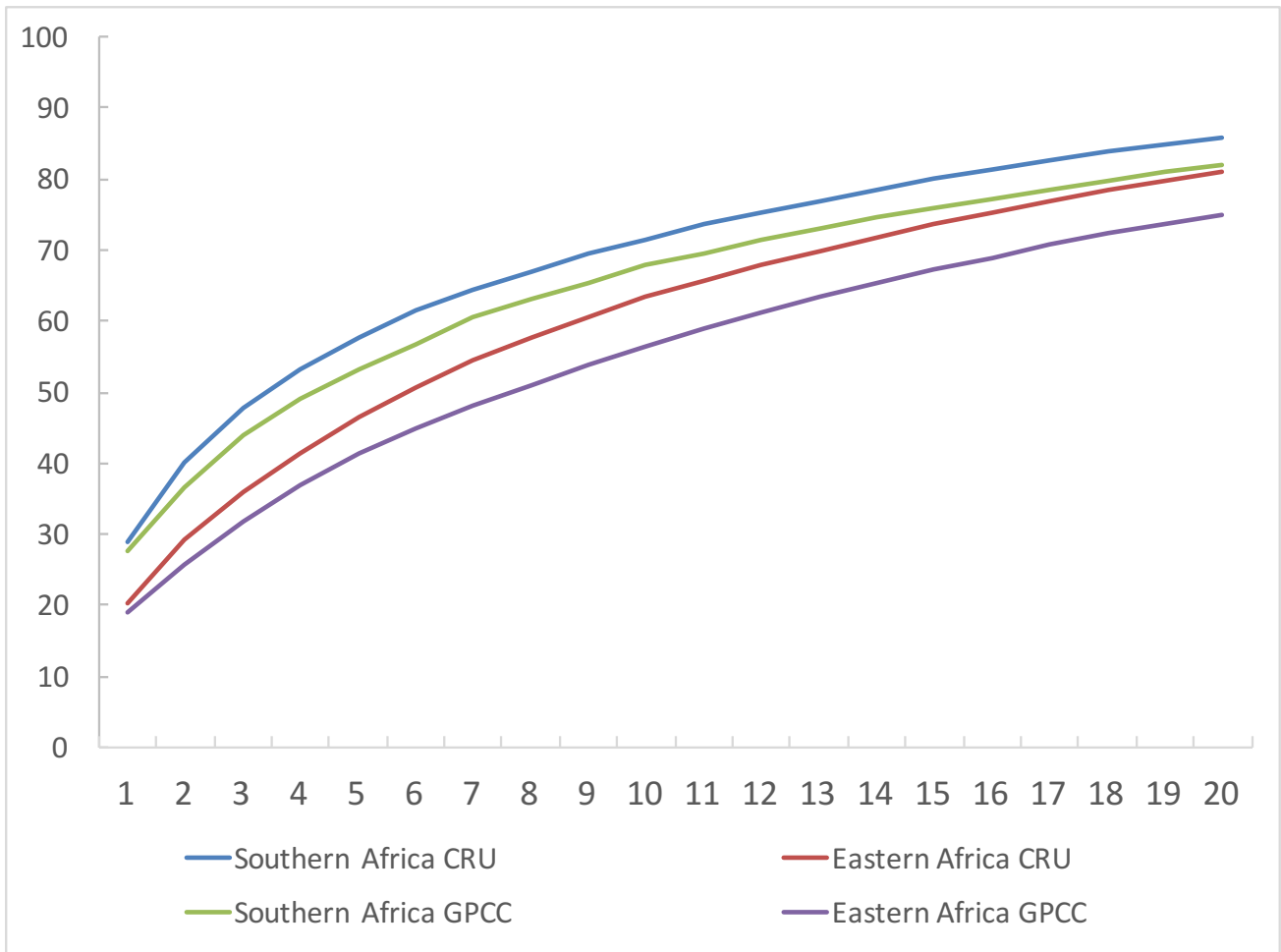
Supplementary Figure 9. Map of seven clusters and main river basin outlines for southern Africa, for analysis period 1956-2011, (a.) CRU TS rainfall data, (b.) GPCP rainfall data. Note the full basin outline shown for the Orange River was not used for calculations and three Pumped Storage Schemes (small basins adjacent to Orange basin) were also not used (See Supplementary Table 17 for list of dams used).



Supplementary Figure 10. Map of three clusters and main river basin outlines for eastern Africa, for analysis period 1956-2011, (a.) CRU TS rainfall data, (b.) GPCC rainfall data.



Supplementary Figure 11: Long-term mean (1956-2011) annual total precipitation (mm/year) across southern and eastern Africa from CRU TS3.24 observations (updated from *1*) with insets showing annual cycles of monthly precipitation (mm/month) for the areas marked in southern and eastern Africa.



Supplementary Figure 12. Share of variance (%) explained by 20 principal components (x-axis) with CRU and GPCP rainfall datasets. Annual for eastern Africa (1956-2011) and July to June for southern Africa (1956/57-2010/11).

	Installed Capacity	% total	New Capacity	% total	Capacity 2030	% total	Year	Per cent of hydropower capacity in cluster			
								G_E3_1	G_E3_2	G_E3_3	All
Whole region	9841	100	24059	100	33900	100	2015	26.1	2.8	71.1	100.0
							2030	19.2	5.8	75.0	99.9
Nile Basin	6116	62.1	21601	89.8	27717	81.8	2015	13.9	0.8	47.5	62.1
							2030	13.2	0.5	68.1	81.8
<i>Main stem</i>	4092	41.6	1840	7.6	5932	17.5	2015	7.6	0.7	33.3	41.6
							2030	3.2	0.3	14.0	17.5
<i>Tekaze</i>	300	3.0	321	1.3	621	1.8	2015	0.0	0.0	3.0	3.0
							2030	0.0	0.0	1.8	1.8
<i>Blue Nile</i>	1094	11.1	12040	50.0	13134	38.7	2015	0.3	0.0	10.8	11.1
							2030	0.6	0.0	38.2	38.7
<i>Baro</i>	-	-	3487	14.5	3487	10.3	2015	-	-	-	-
							2030	0.0	0.0	10.3	10.3
<i>White Nile</i>	630	6.4	1808	7.5	2438	7.2	2015	5.9	0.1	0.4	6.4
							2030	5.8	0.1	1.3	7.2
<i>White Nile BEJ</i>	-	-	2105	8.7	2105	6.2	2015	-	-	-	-
							2030	3.6	0.0	2.5	6.2
Omo	2474	25.1	-	-	2474	7.3	2015	2.0	0.0	23.1	25.1
							2030	0.6	0.0	6.7	7.3
Rufiji	460	4.7	2458	10.2	2918	8.6	2015	3.1	1.5	0.0	4.7
							2030	3.3	5.2	0.0	8.6
Tana	527	5.4	-	-	527	1.6	2015	5.4	0.0	0.0	5.4
							2030	1.6	0.0	0.0	1.6
Other basins	264	2.7	-	-	264	0.8	2015	1.7	0.5	0.4	2.7
							2030	0.5	0.2	0.1	0.8

Supplementary Table 1: Results for eastern Africa using GPCC rainfall clusters: installed capacity (sites > 50 MW) for present (2015) and future (2030). Per cent of total regional capacity is shown by major river basin (sub-basins in italics) and by area of precipitation cluster. White Nile BEJ = White Nile Bahr el Jebel.

Per cent of hydropower capacity in cluster															
	Installed Capacity	% total	New Cap	% total	Total cap 2030	% total	Year	G_S 7_1	G_S7 2	G_S 7_3	G_S7 4	G_S 7_5	G_S 7_6	G_S7 7	All
Whole region	7196	100	7982	100	15178	100	2015	5.3	22.4	8.3	43.6	5.6	2.0	12.7	100
							2030	2.5	16.1	6.2	51.4	9.0	1.0	13.9	100
Zambezi basin	5284	73.4	7643	95.8	12927	85.2	2015	0.0	7.0	7.4	43.4	5.6	0.0	10.1	73.4
							2030	0.0	8.8	5.7	49.4	8.7	0.0	12.7	85.2
<i>Kafue</i>	1020	14.1	870	10.9	1890	12.5	2015	0.0	0.0	0.0	13.4	0.8	0.0	0.0	14.2
							2030	0.0	0.0	0.0	11.7	0.8	0.0	0.0	12.5
<i>Zambezi main Stem</i>	3983	55.4	6093	76.3	10076	66.4	2015	0.0	7.0	7.4	28.3	2.5	0.0	10.1	55.4
							2030	0.0	8.8	5.7	36.3	2.9	0.0	12.7	66.4
<i>Shire</i>	281	3.9	680	8.5	961	6.3	2015	0.0	0.0	0.0	1.6	2.3	0.0	0.0	3.9
							2030	0.0	0.0	0.0	1.4	5.0	0.0	0.0	6.3
Orange	600	8.3	-	-	600	4.0	2015	5.3	0.0	0.5	0.0	0.0	0.0	2.6	8.3
							2030	2.5	0.0	0.2	0.0	0.0	0.0	1.2	4.0
Kwanza	700	9.7	-	-	700	4.6	2015	0.0	9.7	0.0	0.0	0.0	0.0	0.0	9.7
							2030	0.0	4.6	0.0	0.0	0.0	0.0	0.0	4.6
Other basins	612	8.5	339	4.2	951	6.3	2015	0.0	5.7	0.4	0.3	0.0	2.0	0.0	8.5
							2030	0.0	2.7	0.2	2.0	0.3	1.0	0.0	6.3

Supplementary Table 2: Results for southern Africa using GPCC rainfall clusters: installed capacity (sites > 50 MW) for present (2015) and future (2030). Precipitation is calculated from July to June for southern Africa (seven clusters).

	Nino3.4	SOI	IOD	SAM
E3_1	0.22 (-0.04, 0.46)	-0.16 (-0.41, 0.11)	0.40 (0.15, 0.60)	-0.08 (-0.34, 0.19)
E3_2	0.00 (-0.27, 0.27)	0.11 (-0.16, 0.37)	0.18 (-0.09, 0.43)	-0.18 (-0.43, 0.09)
E3_3	-0.29 (-0.52, -0.03)	0.37 (0.11, 0.58)	0.05 (-0.22, 0.31)	0.08 (-0.19, 0.34)

Supplementary Table 3. Three clusters. Correlations computed for period 1956-2011. Correlation (95% confidence range).

	Nino3.4	SOI	IOD	SAM
E5_1	0.02 (-0.25, 0.28)	0.10 (-0.17, 0.36)	0.18 (-0.09, 0.42)	-0.19 (-0.44, 0.08)
E5_2	-0.03 (-0.29, 0.24)	0.09 (-0.18, 0.35)	0.38 (0.12, 0.58)	0.00 (-0.26, 0.27)
E5_3	-0.25 (-0.48, 0.02)	0.33 (0.08, 0.55)	0.03 (-0.24, 0.29)	0.09 (-0.18, 0.35)
E5_4	0.18 (-0.09, 0.42)	-0.13 (-0.38, 0.14)	0.35 (0.09, 0.56)	-0.09 (-0.34, 0.18)
E5_5	0.14 (-0.13, 0.39)	-0.08 (-0.34, 0.19)	0.13 (-0.14, 0.38)	-0.09 (-0.35, 0.18)

Supplementary Table 4. Five clusters. Correlations computed for period 1956-2011. Correlation (95% confidence range).

	Nino3.4	SOI	IOD	SAM
S9_1	-0.28 (-0.51, -0.02)	0.36 (0.10, 0.57)	-0.25 (-0.49, 0.01)	-0.07 (-0.33, 0.20)
S9_2	-0.42 (-0.62, -0.18)	0.49 (0.26, 0.67)	-0.10 (-0.35, 0.17)	0.16 (-0.11, 0.41)
S9_3	-0.40 (-0.60, -0.15)	0.36 (0.11, 0.57)	-0.26 (-0.49, 0.01)	0.12 (-0.15, 0.37)
S9_4	-0.04 (-0.30, 0.23)	0.11 (-0.16, 0.37)	0.10 (-0.16, 0.36)	0.09 (-0.18, 0.35)
S9_5	-0.09 (-0.35, 0.18)	0.15 (-0.12, 0.40)	0.05 (-0.22, 0.31)	-0.23 (-0.47, 0.04)
S9_6	-0.05 (-0.31, 0.22)	-0.04 (-0.30, 0.23)	0.13 (-0.14, 0.38)	0.01 (-0.25, 0.28)
S9_7	-0.06 (-0.32, -0.21)	-0.12 (-0.15, 0.38)	-0.08 (-0.34, 0.19)	-0.21 (-0.45, 0.06)
S9_8	-0.30 (-0.52, -0.03)	0.33 (0.07, 0.55)	-0.24 (-0.47, 0.03)	0.12 (-0.15, 0.37)
S9_9	-0.43 (-0.62, -0.18)	0.44 (0.19, 0.63)	-0.24 (-0.48, 0.02)	0.03 (-0.24, 0.29)

Supplementary Table 5. Nine clusters. Correlations computed for period 1956/57-2011/12. Correlation (95% confidence range).

	Nino3.4	SOI	IOD	SAM
S7_1	-0.39 (-0.60, -0.14)	0.35 (0.10, 0.57)	-0.25 (-0.48, 0.02)	0.12 (-0.15, 0.37)
S7_2	-0.07 (-0.33, 0.20)	0.13 (-0.14, 0.38)	-0.08 (-0.33, 0.19)	-0.20 (-0.44, 0.07)
S7_3	-0.28 (-0.51, -0.01)	0.32 (0.06, 0.54)	-0.22 (-0.46, 0.04)	0.12 (-0.15, 0.37)
S7_4	-0.39 (-0.59, -0.14)	0.43 (0.19, 0.63)	-0.29 (-0.52, -0.03)	-0.04 (-0.31, 0.22)
S7_5	-0.06 (-0.32, 0.21)	0.03 (-0.23, 0.30)	0.12 (-0.15, 0.38)	-0.10 (-0.36, 0.17)
S7_6	-0.15 (-0.40, 0.12)	0.19 (-0.08, 0.44)	0.06 (-0.21, 0.32)	0.09 (-0.18, 0.35)
S7_7	-0.40 (-0.60, -0.16)	0.47 (0.23, 0.65)	-0.13 (-0.38, 0.14)	0.13 (-0.14, 0.38)

Supplementary Table 6. Seven clusters. Correlations computed for period 1956/57-2011/12. Correlation (95% confidence range).

	E3_1	E3_2	E3_3
E3_1	100	58	25
E3_2		100	20

Supplementary Table 7. Three clusters. Correlations computed using data only for 1956-2011. Correlation matrix ($r \times 100$).

	E5_1	E5_2	E5_3	E5_4	E5_5
E5_1	100	26	19	58	42
E5_2		100	26	49	11
E5_3			100	19	27
E5_4				100	39

Supplementary Table 8. Five clusters. Correlations computed using data only for 1956-2011. Correlation matrix ($r \times 100$).

	S9_1	S9_2	S9_3	S9_4	S9_5	S9_6	S9_7	S9_8	S9_9
S9_1	100	69	34	-5	21	-15	31	67	55
S9_2		100	53	11	5	-10	17	63	39
S9_3			100	-18	-9	-23	-12	55	4
S9_4				100	21	19	42	-20	3
S9_5					100	53	44	-5	41
S9_6						100	22	-32	4
S9_7							100	2	13
S9_8								100	54

Supplementary Table 9. Nine clusters. Correlations computed using data only for 1956/57-2011/2. Correlation matrix ($r \times 100$).

	S7_1	S7_2	S7_3	S7_4	S7_5	S7_6	S7_7
S7_1	100	-13	53	38	-18	-12	49
S7_2		100	2	23	35	38	19
S7_3			100	66	-22	-19	66
S7_4				100	12	6	57
S7_5					100	30	-4
S7_6						100	8

Supplementary Table 10. Seven clusters. Correlations computed using data only for 1956/57-2011/2. Correlation matrix ($r \times 100$).

Southern Africa clusters defined on 1981-2011				
Correlations computed for period 1980/1981 - 2011/2012				
	Nino3.4	SOI	IOD	SAM
S7_1	-0.37 (-0.64, -0.02)	0.43 (0.09, 0.68)	-0.01 (-0.36, 0.34)	0.42 (0.08, 0.67)
S7_2	-0.54 (-0.74, -0.23)	0.58 (0.29, 0.77)	-0.03 (-0.38, 0.32)	0.40 (0.06, 0.66)
S7_3	-0.32 (-0.60, 0.04)	0.25 (-0.11, 0.55)	-0.32 (-0.60, 0.03)	-0.02 (-0.37, 0.34)
S7_4	-0.58 (-0.77, -0.29)	0.54 (0.24, 0.75)	-0.23 (-0.54, 0.13)	0.33 (-0.03, 0.61)
S7_5	-0.09 (-0.43, 0.27)	0.16 (-0.20, 0.48)	0.23 (-0.13, 0.54)	0.31 (-0.05, 0.60)
S7_6	-0.25 (-0.55, 0.11)	0.30 (-0.05, 0.59)	-0.05 (-0.39, 0.30)	-0.01 (-0.36, 0.35)
S7_7	0.15 (-0.21, 0.48)	-0.27 (-0.56, 0.09)	-0.02 (-0.37, 0.33)	-0.04 (-0.39, 0.32)
Southern Africa clusters defined on 1951-1980				
Correlations computed for period 1950/1951 - 1980/1981				
	Nino3.4	SOI	IOD	SAM
S7_1	-0.29 (-0.58, 0.07)	0.19 (-0.17, 0.51)	-0.25 (-0.55, 0.12)	0.12 (-0.25, 0.45)
S7_2	-0.31 (-0.60, 0.05)	0.19 (-0.18, 0.51)	-0.11 (-0.44, 0.26)	0.20 (-0.17, 0.52)
S7_3	-0.57 (-0.77, -0.27)	0.58 (0.28, 0.78)	-0.01 (-0.37, 0.34)	0.36 (0.01, 0.63)
S7_4	-0.04 (-0.38, 0.32)	0.24 (-0.12, 0.55)	0.19 (-0.18, 0.51)	0.34 (-0.02, 0.62)
S7_5	0.04 (-0.32, 0.38)	-0.02 (-0.37, 0.34)	0.11 (-0.26, 0.44)	0.10 (-0.26, 0.44)
S7_6	-0.49 (-0.72, -0.16)	0.52 (0.21, 0.74)	-0.28 (-0.58, 0.08)	0.11 (-0.26, 0.45)
S7_7	-0.23 (-0.54, 0.13)	0.27 (-0.10, 0.57)	0.36 (0.01, 0.63)	0.29 (-0.07, 0.58)

Supplementary Table 11. As Supplementary Table 4 but with clusters defined on two shorter periods / correlations with modes of climate variability calculated on two shorter periods. Note that the numbering of clusters is an arbitrary outcome of the clustering algorithm and varies between each case, so refer to Supplementary Figure 7 to identify which cluster numbers represent the most closely co-located regions between each case.

Eastern Africa clusters defined on 1981-2011				
Correlations computed for period 1980 - 2011				
	Nino3.4	SOI	IOD	SAM
E3_1	-0.01 (-0.36, 0.34)	0.09 (-0.26, 0.43)	0.14 (-0.22, 0.46)	0.03 (-0.33, 0.37)
E3_2	0.31 (-0.04, 0.60)	-0.21 (-0.52, 0.15)	0.48 (0.16, 0.71)	0.16 (-0.20, 0.48)
E3_3	-0.40 (-0.66, -0.07)	0.45 (0.12, 0.69)	0.27 (-0.09, 0.57)	0.42 (0.09, 0.67)

Eastern Africa clusters defined on 1951-1980				
Correlations computed for period 1950 - 1980				
	Nino3.4	SOI	IOD	SAM
E3_1	-0.03 (-0.38, 0.32)	0.03 (-0.33, 0.38)	0.38 (0.03, 0.65)	0.23 (-0.13, 0.54)
E3_2	0.31 (-0.05, 0.60)	-0.29 (-0.59, 0.07)	0.53 (0.21, 0.74)	-0.05 (-0.40, 0.31)
E3_3	-0.13 (-0.47, 0.23)	0.16 (-0.21, 0.49)	-0.06 (-0.41, 0.30)	0.02 (-0.34, 0.37)

Supplementary Table 12. As Supplementary Table 7 but with clusters defined on two shorter periods / correlations with modes of climate variability calculated on two shorter periods. Note that the numbering of clusters is an arbitrary outcome of the clustering algorithm and varies between each case, so refer to Supplementary Figure 8 to identify which cluster numbers represent the most closely co-located regions between each case.

	Southern Africa CRU	Southern Africa GPCC	Eastern Africa CRU	Eastern Africa GPCC
1	28.76	27.64	20.38	18.95
2	40.04	36.59	29.21	25.71
3	47.70	43.89	35.80	31.83
4	53.24	48.99	41.46	37.06
5	57.75	53.07	46.43	41.31
6	61.48	56.84	50.77	44.87
7	64.37	60.42	54.47	47.97
8	67.05	62.98	57.70	50.95
9	69.43	65.48	60.66	53.78
10	71.57	67.78	63.33	56.36

Supplementary Table 13. Cumulative share of variance (%) explained by the first ten principal components. Annual for eastern Africa (1956-2011) and July to June for southern Africa (1956/57-2010/11).

Sources and references for existing hydropower sites

- Cervigni, R.; Liden, M. J. R.; Neumann, J. L.; Strzepek, K. M. 2015. Enhancing the climate resilience of Africa's infrastructure : the power and water sectors. Africa Development Forum. Washington, D.C. : World Bank Group.
<http://documents.worldbank.org/curated/en/2015/04/24424659/enhancing-climate-resilience-africas-infrastructure-power-water-sectors>
- ESCOM, Electricity Supply Corporation of Malawi 2015. Accessed 25 November 2015, <http://www.escom.mw/generation.php>
- HydroWorld.com 2015. Power generation begins at 1,870-MW Gibe III hydroelectric project in Ethiopia. Addis Ababa, Ethiopia. Accessed 25 November 2015, <http://www.hydroworld.com/articles/2015/10/power-generation-begins-at-1-870-mw-gibe-iii-hydroelectric-project-in-ethiopia.html>
- Power-technology.com 2015. Bujagali Falls Hydropower Dam, Jinja, Uganda. Accessed 25 November 2015, <http://www.power-technology.com/projects/bujagali/>
- Power-technology.com 2015. Ingula Pumped Storage Scheme, South Africa. Accessed 25 November 2015, <http://www.power-technology.com/projects/ingula-scheme/>
- Darbourn, K. 2015. Impact of the failure of the Kariba dam. Accessed 21 November 2015, https://www.aon.co.za/Assets/docs/general/Kariba_Report.pdf
- LHDA, Lesotho Highlands Water Project Phase 1 2015. Accessed 21 November 2015, http://www.lhda.org.ls/Phase1/?page_id=733;
<http://www.worldbank.org/projects/P001396/lesotho-highlands-water-project-phase-1a?lang=en>
- Global Energy Observatory 2015. Accessed 21 November 2015, <http://GlobalEnergyObservatory.org/>
- World Energy Council. Energy sources 2015. Accessed 21 November 2015, <https://www.worldenergy.org/data/resources/region/africa/hydropower/>
- TANESCO, Tanzania Electric Supply Company Limited 2015. Accessed 25 November 2015, http://www.tanESCO.co.tz/index.php?option=com_content&view=article&id=81&Itemid=237
- Bujagali Energy Limited. Bujagali Hydropower Project, Uganda. Accessed 25 November 2015, <http://www.bujagali-energy.com/>
- KenGen, Kenya Electricity Generating Company Limited 2015. Accessed 25 November 2015, <http://www.kengen.co.ke/index.php?page=business&subpage=hydro>
- UEGCL, Uganda Electricity Generation Company 2015. Accessed 25 November 2015, Limited <http://uegcl.com/>

Sources and references for proposed hydropower sites

- De Condappa, D. and J. Barron (2013), Assessment of Existing and Planned Irrigated Areas in the Congo, Niger, Nile, Orange, Senegal, Volta and Zambezi River Basins; Stockholm Environment Institute Working Paper No 2013-04.
- EAPP/EAC (2011): Regional Power system Master plan and Grid Code Study: Vol. i & iv, May, 2011; Snc Lavalin International Inc. in association with Parsons Brinckerhoff, May 2011, Addis Ababa, Ethiopia. Accessed 21 November 2015
- EPPCO (2013): Ethiopian Power System Expansion Master Plan Study, Interim Report, Vol. 1-3, Nov.2013, Parsons Brinckerhoff, Addis Ababa, Ethiopia.
- HydroWorld.com 2013. Zambia extends EPC contractor call for 750-MW Kafue Gorge Lower hydro development project. Lusaka, Zambia. Accessed 25 November 2015, <http://www.hydroworld.com/articles/2013/06/zambia-extends-epc-contractor-call-for-750-mw->

[kafue-gorge-lower-.html](#)

International Hydropower Association. 2015 Hydropower status report. Accessed 21 November 2015, <https://www.hydropower.org/2015-hydropower-status-report>

International Hydropower Association. Country Profiles. Accessed 21 November 2015, <https://www.hydropower.org/country-profiles>

Miketa, A. and Merven, B. (2013). Southern African Power Pool: Planning and Prospects for Renewable Energy, IRENA. Accessed 21 November 2015, <http://www.irena.org/documentdownloads/publications/sapp.pdf>

Ministry of Energy and Minerals – Tanzania (2013): Power System Master Plan 2012 update, Dar es Salaam, Tanzania. Accessed 21 November 2015

Ministry of Water and Energy – Ethiopia (2014). Dams and Hydropower. Accessed 21 November 2015, <http://www.mowr.gov.et/index.php?pagenum=4.3&pagehgt=1000px>

State of the River Nile Basin (2012). Hydropower Potential and the Region's Rising Energy Demand. Accessed 21 November 2015, <http://nileis.nilebasin.org/system/files/Nile%20SoB%20Report%20Chapter%206%20-%20Hydropower.pdf>

UEGCL, Uganda Electricity Generation Company 2015. Accessed 25 November 2015, Limited <http://uegcl.com/>

World Bank. 2010. Zambezi Basin Multi-Sector Investment Opportunity Analysis (MSIOA) 2010. The World Bank Africa Region. Water Resources Management. Accessed 14 November 2015, http://siteresources.worldbank.org/INTAFRICA/Resources/Zambezi_MSIOA_-_Vol_1_-_Summary_Report.pdf

Zambezi River Authority (2015). Hydro-Electric Schemes. Accessed 21 November 2015, <http://www.zaraho.org.zm/hydro-electric-schemes>

Articles mentioned by Cervigni et al. (2015) unavailable online

NBI-RPT-P (2011): Comprehensive Basin-Wide Study of Power Development Options and Trade Opportunities (Final Report), Dar es Salaam, Tanzania

NBI-NELSAP (2012): Nile Equatorial Lakes-Multi Sector Investment Opportunity Situational Analysis, Situation Analysis Report, Analytic Framework and Investment Strategy and Action Plan

NBI-ENTRO (2009): Eastern Nile Irrigation and Drainage Study, Phase 1 - Diagnostic and Planning and Cooperative Regional Assessment Reports, Eastern Nile Technical Regional Office (ENTRO), Addis Ababa, Ethiopia

NBI-ENTRO (2007): Eastern Nile Power Trade Investment Program Study reports, Eastern Nile Technical Regional Office.

Supplementary Table 14. Sources and references for existing and proposed hydropower sites.

Country	River	Name of dam	Lon	Lat	Installed capacity (MW)	% regional HP
Whole region					9841	100.00
Nile Basin					6115	62.15
Main stem					4092	41.58
Egypt	Main Nile	High Aswan Dam	32.88	23.97	2100	21.34
Egypt	Main Nile	Aswan Dam 1	32.86	24.03	322	3.27
Egypt	Main Nile	Aswan Dam 2	32.86	24.03	270	2.74
Egypt	Main Nile	Esna (Isna)	32.55	25.31	86	0.87
Egypt	Main Nile	Nagaa Hamadi	32.14	26.15	64	0.65
Sudan	Main Nile	Merowe	31.99	18.72	1250	12.70
Ethiopia	Tekeze (Atbara)	Tekeze/ TK5	38.71	13.3	300	3.05
Blue Nile					1094	11.12
Sudan	Blue Nile	Roseires	34.39	11.8	415	4.22
Ethiopia	Fincha Blue Nile	Fincha	37.37	9.56	134	1.36
Ethiopia	Blue Nile	Tana Beles	37.21	11.68	460	4.67
Ethiopia	Blue Nile	Tis Abbay I and II	37.59	11.48	85	0.86
White Nile					630	6.40
Uganda	Victoria Nile	Kiira/ Kiyira	33.18	0.45	200	2.03
Uganda	Victoria Nile	Bujagali	33.13	0.49	250	2.54
Uganda	Victoria Nile	Nalubaale (Owen falls)	33.18	0.44	180	1.83
Omo					2474	25.14
Ethiopia	Gilgel Gibe	Gilgel Gibe I	37.39	7.93	184	1.87
Ethiopia	Gilgel Gibe	Gilgel Gibe II	37.56	7.75	420	4.27
Ethiopia	Omo	Gilgel Gibe III	37.3	6.84	1870	19.00
Other basins					264	2.68
Ethiopia	Awash	Koka	39.16	8.47	43	0.44
Ethiopia	Wabi Shebele	Melka Wakena	39.43	7.17	153	1.55
Tanzania*	Pangani	Pangani falls	38.65	-5.35	68	0.69
Tana					527	5.36

Kenya	Tana	Gitaru	37.68	0.81	225	2.29
Kenya	Tana	Kaimbere	37.91	-0.64	168	1.71
Kenya	Tana	Kindaruma	37.81	-0.81	40	0.41
Kenya	Tana	Kamburu	37.69	-0.81	94	0.96
Rufiji					460	4.67
Tanzania	Great Ruaha	Mtera	35.99	-7.14	80	0.81
Tanzania	Kihansi	Kinhansi/ Lower Kihansi	36.35	-8.40	180	1.83
Tanzania	Great Ruaha	Kidatu	36.91	-7.64	200	2.03

Supplementary Table 15: Eastern Africa, all dams considered in analysis with installed capacity (sites > 50 MW) for existing developments (2015). Rows highlighted in grey are the main river basins for which results are presented in Tables 1 and 2.

Country	River	Name of dam	Lon	Lat	Installed capacity (MW)	% regional HP
Whole region					24059	100.00
Nile Basin					21601	81.76
Main stem					1840	17.50
Sudan	Nile	Dagash	33.32	19.52	320	0.94
Sudan	Nile	Kajbar	30.35	19.78	360	1.06
Sudan	Nile	Low Dal	30.58	21.01	620	1.83
Sudan	Nile	Sabloka	32.6	16.26	120	0.35
Sudan	Nile	Shereiqa	33.55	18.8	420	1.24
White Nile Bahr el Jebel (BEJ)					2105	6.21
South Sudan	Bahr el Jebel	Bedden	31.57	4.66	570	1.68
South Sudan	Bahr el Jebel	Fula	31.88	3.79	890	2.63
South Sudan	Bahr el Jebel	Lakki	31.68	3.97	410	1.21
South Sudan	Bahr el Jebel	Shukoli	31.79	3.87	235	0.69
Ethiopia	Tekeze	Tekeze			321	1.83
Ethiopia	Tekeze	Tekeze II/TK7	38.71	13.3	321	0.95
Blue Nile					12040	38.74
Ethiopia	Didessa	Lower Didessa	35.68	9.94	300	0.88
Ethiopia	Blue Nile	Grand Renaissance Kara	35.09	11.21	6000	17.70
Ethiopia	Blue Nile	Dobe/Karadobi	37.67	9.86	1600	4.72
Ethiopia	Blue Nile	Mandaya	36.44	10.45	2200	6.49
Ethiopia	Blue Nile	Beko Abo	37.01	10.29	1940	5.72
Baro					3487	10.29
Ethiopia	Baro	Baro 2	34.93	8.20	500	1.47
Ethiopia	Birbir	Birbir R	34.98	8.29	465	1.37
Ethiopia	Geba	Geba I II	35.34	8.07	1462	4.31
Ethiopia	Baro	Tams	34.59	8.25	1060	3.13
White Nile					1808	7.19
Uganda	Victoria Nile	Ayago	31.92	2.36	600	1.77
Uganda	Victoria Nile	Isimba	33.00	0.88	183	0.54

Uganda	Victoria Nile	Karuma	32.25	2.25	600	1.77
Uganda	Victoria Nile	Kiba	31.92	2.37	288	0.85
Kenya	Itare	Magwag-wa	35.03	-0.48	120	0.35
Tanzania	Kagera	Kakono	31.42	-1.25	53	0.16
Tanzania	Kagera	Rusumo Falls/ Russomo	30.78	-2.38	84	0.25
Rufiji					2458	8.61
Tanzania	Rufiji	Stiegler's Gorge I II III	38.42	-8.11	2100	6.19
Tanzania	Ruhudji	Ruhudji	35.37	-9.52	358	1.06
Omo		Only current dams			2474	7.30
Tana		Only current dams			527	1.56
Other basins		Only current dams			264	9.63
DRC/ Rwanda	Lake Kivu	Ruzizi III	28.9	-2.6	270	0.80
Tanzania	Rumakali	Rumakali	34.07	-9.21	222	0.65

Supplementary Table 16: Eastern Africa, all planned developments (2030) considered in analysis with planned capacity > 50 MW. Rows highlighted in grey are the main river basins for which results are presented in Tables 1 and 2.

Country	River	Name of dam	Lon	Lat	Installed capacity (MW)	% regional HP
Whole region					7195	100
Zambezi					5283	73.43
Kafue					1020	14.18
Zambia	Kafue	Itehzi - Tehzi	26.02	-15.76	120	1.67
Zambia	Kafue	Kafue Gorge Upper	28.42	-15.81	900	12.51
Main stem					3983	55.35
Zambia	Zambezi	Victoria Falls	25.86	-17.93	108	1.50
Zambia	Zambezi	Kariba Dam North	28.76	-16.52	720	10.01
Zimbabwe	Zambezi	Lake Kariba/ Kariba dam	28.76	-16.52	1080	15.01
Mozambique	Zambezi	Cahora Bassa (HCB South Bank)	32.71	-15.59	2075	28.84
Shire river					280	3.90
Malawi	Shire	Nkhula Falls/Nkula	34.82	-15.51	124	1.72
Malawi	Shire	Kapichira	34.75	-15.89	64	0.89
Malawi	Shire	Tedzani	34.78	-15.55	92	1.29
Orange					600	8.34
South Africa	Orange	Gariep	25.50	-30.62	360	5.00
South Africa	Orange	Van der kloof	24.73	-29.99	240	3.34
Kwanza					700	9.73
Angola	Kwanza	Cambambe	14.48	-9.75	180	2.50
Angola	Kwanza	Capanda	15.46	-9.79	520	7.23
Other basins					612	8.51
Angola	Cunene	Gove	15.87	-13.45	320	4.45
Mozambique	Buzi	Mavuzi	33.49	-19.52	52	0.72
Namibia	Kunene	Ruacana	14.22	-17.38	240	3.34

Supplementary Table 17: Southern Africa, all dams considered in analysis with installed capacity (sites > 50 MW) for existing developments (2015). Rows highlighted in grey are the main river basins for which results are presented in Tables 1 and 2.

Country	River	Name of dam	Lon	Lat	Installed capacity (MW)	% regional HP
Whole region					7982	100
Zambezi					7643	85.17
Kafue					870	12.45
Zambia	Kafue	Kafue Gorge Dam Lower	28.42	-15.81	750	4.94
Zambia	Kafue	Itezhi – Tezhi	26.02	-15.76	120	0.79
Main stem					6093	66.39
Zambia/Zimbabwe	Zambezi	Devils Gorge	26.86	-17.99	1240	8.17
Zambia/Zimbabwe	Zambezi	Kariba North Extension	28.76	-16.52	360	2.37
Zambia/Zimbabwe	Zambezi	Mpata Gorge	32.03	-13.30	543	3.58
Zimbabwe	Zambezi	Batoka Gorge	26.13	-17.92	1600	10.54
Mozambique	Zambezi	Mphanda Nkuwa	33.43	-16.00	1500	9.88
Zambia	Zambezi	HCB North Bank	32.71	-15.59	850	5.60
Shire river					680	6.33
Malawi	Shire	Khlolombizo	35.26	-14.46	240	1.58
Malawi	Songwe	Songwe I, II, and III	33.62	-9.60	340	2.24
Malawi	Rukuru	Lower Fufu	34.19	-10.76	100	0.66
Other basins					339	14.83
Zambia	Lusemfwe	Lunsemfwa Expansion/Muchinga Hydro Power	28.84	-14.73	255	1.68
Zambia	Lusiwasi	Lusiwasi	31.27	-13.44	84	0.55

Supplementary Table 18: Southern Africa, all planned developments (2030) considered in analysis with planned capacity > 50 MW. Rows highlighted in grey are the main river basins for which results are presented in Tables 1 and 2.

Supplementary Note 1: Southern Africa full results; 1956/57-2010/11

Supplementary Figure 2 shows the clusters as defined on the CRU TS 0.5° grid for 9 (S9_1 to S9_9) and 7 (S7_1 to S7_7) clusters, respectively. The cluster number is used for the timeseries analyses shown below, so it is labelled on each figure to enable identification. With a few minor exceptions, the clusters are contiguous and show some agreement with expected climate regimes – though note that the clusters are determined by common year-to-year variability rather than by similar climatological means.

The regionalisation is quite stable between these two versions, with most clusters very similar and the main differences are that clusters S9_5 and S9_6 (in the nine cluster case) are combined to form cluster S7_5 (in the seven cluster case) and cluster S9_1 is split, with half joining S9_9 to form S7_4 and the remainder joining S9_2 to form S7_7.

Supplementary Figures 3 and 4 show the timeseries of annual-mean precipitation (from CRU TS3.24) for the 9 and 7 clusters, respectively. Some clusters show strong multidecadal variability, and particular extreme events are evident in all cases. By reference to the different cluster numbering (Supplementary Figure 2), it is clear that the small differences in regional definitions make little difference to the regional timeseries and that the combined regions for the seven cluster case do have some common variability when kept separate in the nine cluster case.

Artefacts of incomplete data coverage are also present, and guide further analysis of these clusters. The CRU TS gridded precipitation values are relaxed towards their climatological mean when there are no nearby weather stations (and are held constant at the climatological mean when there are no stations within the correlation decay distance, which for precipitation is 450 km; *I*). This is manifest as suppressed variability and a return to the 1961-1990 climatological mean and is particularly apparent after about 1995 in clusters S9_4, S9_7, S7_2 and S7_6, reflecting less data availability from Angola for recent years in the CRU TS database. Although less apparent in these timeseries, the number of African precipitation stations available in the first few decades of the twentieth century is relatively low (see *I*). The period with best overall data coverage is 1931 to 1995.

Although the cluster analysis, by building on the underlying PCA, groups grid cells with similar correlations and excludes grid cells with dissimilar correlation, it is nevertheless the case that there will be intra-cluster variation and there will be correlated behaviour between clusters. The choice of how many clusters to define is, therefore, somewhat arbitrary – though guided by knowledge of different regional climate regimes and by a preference for spatially contiguous regions. Choosing fewer clusters might overstate the coherent variability (and thus exposure to concurrent climate risk) by combining grid cells with increasing amounts of independent variability into single clusters, whereas choosing more clusters might understate the coherent variability because separate clusters may nevertheless be significantly correlated with each other. A further issue is that the strength of spatial correlations may vary over time (due to random sampling variability, due to changing strength of common external drivers, or due to dataset artefacts), making the results sensitive to the period of analysis. These issues are explored by considering the matrices of correlations between regions for different time periods and for the nine and seven cluster choices.

Considering first the period over which the clusters were defined (1956/7 to 2011/2), $r > 0.5$ occurs (Supplementary Table 1) between eight cluster pairs: (S9_1, S9_2) (S9_1, S9_8) (S9_1, S9_9) (S9_2, S9_3) (S9_2, S9_8) (S9_3, S9_8) (S9_5, S9_6) and (S9_8, S9_9). It is not surprising that two

of these pairs (S9_1, S9_2) and (S9_5, S9_6) are joined when only seven clusters are defined. With seven clusters (Supplementary Table 2), only four pairs of regions have $r > 0.5$, the adjacent (see Fig. 2 in the main paper) pairs (S7_1, S7_3) (S7_3, S7_4) (S7_3, S7_7) and (S7_4, S7_7).

Inter-regional correlations computed over the longer (1931/2 to 2011/2) period with reasonable data coverage (not shown) have a similar number of strong inter-cluster correlations: with nine clusters, $r > 0.5$ occurs for the same eight regions, while with seven clusters there are only three pairs with $r > 0.5$, namely (S7_1, S7_3) (S7_3, S7_4) and (S7_3, S7_7).

The mechanisms that cause spatial coherence in the precipitation fields (both the spatial coherence that allows these cluster regions to be defined, and also that contributes to these correlations between clusters) include the inherent spatial scale of individual weather systems as they cross southern Africa and the common “external” drivers of rainfall variability. Here, we consider correlations between these cluster area-average, annual-mean precipitation time series and four indices describing modes of climate variability: two measuring El Niño Southern Oscillation (ENSO) variability – the Nino3.4 sea surface temperature and the Southern Oscillation Index (SOI) – one measuring Indian Ocean variability – the Indian Ocean Dipole (IOD) – and one measuring Southern Hemisphere extratropical variability – the Southern Annular Mode (SAM).

Supplementary Tables 5 and 6 show the correlations for the nine and seven clusters for the period over which the clustering was done (1956/7 to 2011/2), which is almost the same period for which the SAM data is considered to be reasonable (1957/8 to 2011/2) according to (2). See Supplementary Note 3 for results using different time periods. The 95% confidence interval is given to highlight the likely range of genuine correlation, and correlations are different from zero with statistical significance when this range does not encompass zero (highlighted bold). The confidence intervals are calculated for data without autocorrelation (they would be wider for series with autocorrelation) but the best estimates would not be affected and this is sufficient for our purposes here, which is a simple exploration of the reasons for coherent precipitation across the region.

Data sources:

Nino3.4: from HadISST1 http://www.esrl.noaa.gov/psd/gcos_wgsp/Timeseries/Nino34/

SOI: Tahiti-Darwin SLP from CRU <https://crudata.uea.ac.uk/cru/data/soi/>

IOD: Dipole Mode Index (DMI)

http://www.jamstec.go.jp/frcgc/research/d1/iod/iod/dipole_mode_index.html

SAM: from 20CRV2c reanalysis

http://www.esrl.noaa.gov/psd/data/20thC_Rean/timeseries/monthly/SAM/

Guided by previous analyses, the following seasonal averages were used for each index (always correlated against the July-June annual-mean precipitation for the concurrent year, there are no lags):

Nino3.4: DJF

SOI: DJF

IOD: July-June

SAM: July-June

Regional precipitation is correlated negatively with Nino3.4 and positively with SOI (except for two northern regions for the nine-cluster case) across the whole southern African domain. This consistency demonstrates field significance and agrees with the expectation of drier conditions associated with El Niño events in this domain. The weakest (and non-significant) correlations are with the northern clusters (S9_4, S9_5, S9_6, S9_7 for nine clusters; S7_2, S7_5, S7_6 for seven clusters) and the strongest are with the southern and southeastern clusters. They are fairly stable

between analysis periods (see Section SI-3, though the southeastern clusters S9_8 and S7_3 are less strongly correlated with ENSO in the more recent period). This ENSO influence explains why precipitation variability is coherent in these regions, and also between some of the region's pairs (see earlier discussion of the strongest inter-cluster correlations).

Correlations with IOD are weaker, as expected because the IOD influence is stronger in eastern Africa rather than southern Africa (Figure 4 of 3; see also 4, 5). There are some mainly negative correlations (drier conditions associated with positive IOD DMI, a greater SST gradient from west to east in the Indian Ocean) in the south and east, e.g. for the southernmost region (S9_3 for nine clusters, S7_1 for seven clusters) in agreement with September-November rainfall anomalies shown in Figure 4 of (3) and one or two other clusters in the east (e.g. statistically significant for S7_4 over parts of Zambia and Zimbabwe).

The SAM index is not very well constrained by observations prior to the 1950s. For the period over which the clusters were defined, there are no significant correlations with the SAM index. For the shortest analysis period considered in Supplementary Note 3, 1980/1 to 2011/2, there are moderate positive correlations with SAM across some western and southern clusters (S9_2, S9_4 and S9_8 for nine clusters; S7_3, S7_6 and S7_7 for seven clusters) but excluding the southernmost cluster (Western and Eastern Cape, S9_3 for nine clusters and S7_1 for seven clusters). This is partly in agreement with Fig. 1c of (2), except that they also find a positive correlation with precipitation over the Eastern Cape and their correlations remain for a longer period beginning from 1957/8, whereas the correlations with regional-average precipitation weaken for the longer period. Note that (2) analysed smaller temporal and spatial scales (individual monthly anomalies for individual weather stations) than those considered here.

Supplementary Note 2: Eastern Africa full results; 1956-2011

The analysis was repeated for the eastern African regions defined by cluster analysis, comparing three and five cluster regions. See maps and time series in Supplementary Figures 4-6. Inter-cluster correlations again show stronger inter-cluster correlations for longer analysis periods than for shorter periods, and correlations for the period over which the cluster analysis was done (Supplementary Tables 5-6) have one cluster pair whose correlation exceeds 0.5 in each case. The most northwesterly cluster in each case (stretching from the southeast Sahel down towards the Ethiopian highlands) shows the weakest correlations with others, so it has more independent variability than the others.

With three clusters (Supplementary Table 3), regional annual precipitation shows significant correlations with ENSO and with IOD that are consistent across the different analysis periods considered here and with prior work (e.g. 6). As expected due to its lack of proximity, correlations with SAM are weak and the only significant correlations (for one period only, 1980-2011) are likely to be due to chance given that they change sign for the longer analysis periods. Cluster E3_2 is not significantly correlated with any of the indices considered here for 1956-2011. Wetter conditions in cluster E3_1 (countries with Indian Ocean coastlines) are associated with positive IOD DMI and with warm (El Niño) ENSO events (not significantly for 1956-2011, but significantly for longer analysis periods), consistent with prior studies (4; 5).

There is an opposite relationship for cluster E3_3 (SE Sahel and part of the Ethiopian highlands), with drier conditions associated with warm (El Niño) events. This is consistent with the 2015 drought coinciding with the 2015 El Niño event (7). The relationship is consistently strong across most analysis periods and using either Nino3.4 or SOI indices and so it is more likely that it is a genuine association with ENSO and is consistent with studies of precipitation teleconnections in Ethiopia and flows of the Blue Nile that drains a large part of this cluster area (8; 9).

Separating the rainfall into five cluster regions instead of three yields similar results (Supplementary Table 3). Cluster E3_2 in the three-cluster case is approximately split into Clusters E5_1 and E5_5 in the five-cluster case, and these remain mostly uncorrelated with the indices considered here.

Cluster E3_1 in the three-cluster case, which was positively correlated with Nino3.4 and with IOD, is approximately split into clusters E5_2 and E5_4 in the five cluster case (though cluster E5_5 also encroaches slightly on the three-cluster cluster E3_1). This separation has weakened the positive correlations with Nino3.4 and IOD and shows that the ENSO influence arises more strongly from the southern area (five-cluster cluster E5_4) and less so from E5_2, the northern part of the Horn of Africa, whereas the IOD influence is more evenly associated with both regions.

Cluster E3_3 in the three-cluster case is approximately the same as cluster E5_3 in the five-cluster case, and maintains the negative correlations with Nino3.4 and the positive correlations with SOI that were commented on above. They are slightly weakened across all periods considered and across both indices, compared with E3_3.

Supplementary Note 3: Temporal stability of clusters and correlations

To examine the temporal stability of the clusters and teleconnections we defined clusters using several alternative periods; 1951-1980, 1981-2011 and as described above 1956-2011. The cluster definitions are more sensitive to analysis period for southern Africa (Supplementary Figure 7; compare also with the right panel of Supplementary Figure 2) than for eastern Africa (Supplementary Figure 8; compare with the left panel of Supplementary Figure 5). The three clusters in eastern Africa divide the region into similar regions (northwest, east and south) regardless of analysis period. For southern Africa, some features are insensitive to analysis period (e.g. the western and eastern Cape) whereas further north there is more similarity between the earlier period (1951-1980) and the longer period (1956-2011) than with the later period (1981-2011).

The correlations between clusters and key climate indices of large-scale variability for both periods are shown for the periods 1951-1980, 1981-2011 in Supplementary Table 11 for southern Africa (compare with Supplementary Table 4 for the longer period) and in Supplementary Table 12 for eastern Africa (compare with Supplementary Tables 3 and 6 for the longer period). In southern Africa, nearly all the regional rainfall series are negative correlated with Nino3.4 (and positively with SOI) even when clusters are defined and correlations evaluated over short periods. The differences in the correlations with ENSO are less marked than for the IOD. For the latter, there are no statistically significant IOD correlations using the 1951-1980 cluster timeseries, whereas one region (S7_7) does for the clusters defined on 1981-2011.

In eastern Africa, the significant correlation between the IOD and the precipitation in the easternmost cluster (E3_2 for the shorter period; Supplementary Figure 8) is apparent for both periods, while the correlation with ENSO is significant only for the later period (Supplementary Table 12). Opposite ENSO influences for clusters 1981-2011 E3_2 and E3_3 are smeared together in the spatial cluster configurations defined for 1951-1980, leaving hardly any correlation with ENSO in the earlier period.

Supplementary Figure 7 shows the correspondence between the southern Africa spatial patterns for the different cluster definitions and the hydropower infrastructure. The 1951-1980 clusters are split across the main hydropower generating basin (the Zambezi) whereas a much higher concentration of hydropower occurs in one rainfall cluster (S7_6) using the period 1981-2011.

As noted above, the cluster patterns for eastern Africa are much more stable between the 1951-1980 and 1981-2011 periods. The main difference is greater coverage of DRC and less coverage of northern Lake Victoria in cluster E3_2 between the 1951-1980 and 1981-2011 periods.

The strength of spatial correlations varies over time due to random sampling variability, probably contributing to the sensitivity of cluster definitions in southern Africa discussed above, between the two shorter analysis periods. This provides justification for defining clusters using the longest possible period of reliable data. Taking 1951-2011 would maximise sample size and hence minimise sampling variability. The strength of spatial correlations may also vary over time due to changing strength of common external drivers. For this possibility, we are guided by previous analyses, in particular Richard et al. (2000). They found a substantial change in ENSO correlation (from weak to strong association) with southern African rainfall using a 20-year sliding window when centred on 1965 [the period 1956-1975]. This suggests avoiding any data prior to 1956 in defining the clusters.

We therefore decided to use the period 1956-2011 to define the clusters; this reduces sampling variability (by using a longer period) and reduces any influence of changing ENSO teleconnection on southern Africa.

Supplementary Note 4: Central Africa and the Grand Inga dam

Several phases of a mega-project are planned to develop the Grand Inga dam in the Democratic Republic of Congo (DRC) up to a potential installed capacity of 39,000 MW by 2030 (Fig. 1). This is greater than the total planned in eastern and southern Africa combined (Tables 1 and 2). The pace of future infrastructure development in DRC is highly uncertain, but, if completed, Grand Inga would change the dynamics of electricity generation and energy security across much of Africa. Completion would greatly increase the potential for power sharing and for Power Pools to spread risk of concurrent electricity outages. To examine this we used the good quality long record of Congo river discharge (gauge located at Kinshasa) to provide a proxy for interannual rainfall variability in the basin (record available for 1903-96) and compared it with river discharge series in eastern and southern Africa. We excluded Central Africa from our Principal Components Analysis of precipitation due to the very poor coverage of rain gauges. Just 0–5 gauges are operational in the Congo basin in the CRU TS data set during the 1980s and 1990s (11) and the fractional coverage across Central Africa of CRU grid squares containing at least one gauge falls from roughly 80% during 1985-1990 to less than 20% during 1997-2010 (12). Good quality long river flow series are available for the Blue Nile and the White Nile (as outflows from Lake Victoria) and the upper Zambezi. The discharge series have been described and analysed extensively (11). For the other (generally much smaller) rivers with hydropower dams the flow records are short, affected by human activities and/or poor quality. The results are included in the main paper (Fig. 3).

Supplementary Note 5: Variance explained by principal components

The cumulative variance accounted for by the principal components in each region is shown in Figure S12 (see also Supplementary Table 13). With CRU rainfall data the first principal components account for 29% and 20% in southern and eastern Africa, respectively. In the main paper, results are presented for CRU data with seven principal components in southern Africa, accounting for 64% of the total variance (69% is accounted for with nine principal components). Results for eastern Africa with three principal components are considerably lower 36% (46% with five). Results are similar between the CRU and GPCC datasets. This is likely due to the stronger diversity of seasonal precipitation (unimodal in the north and south, bi-modal across much of the central parts of the region), and contrasting teleconnection influences during each seasonal maxima. The scree plot is used as one of the many ways to decide when to stop the selection of the number of PCs. The selection of the number of PCs is justified through the physical sense of the cluster teleconnections and that the maps are similar to the ones captured in other studies using PCA in SSA.

Supplementary Note 6: Collection and categorization of existing and proposed hydropower sites in eastern and southern Africa

Data collection was carried out for two types of hydropower sites: (i) existing and (ii) proposed. Only those sites with more than 50 MW installed capacity are included in this study.

For information on existing hydropower sites, our primary source of data is a recent World Bank study (13) from which details of hydropower sites in Eastern and Southern Africa are collected. Cervigni et al. (13) provide details regarding existing as well as proposed sites based on key documents and reports prepared by governments and other agencies. Some hydropower sites and related information not mentioned in (13) were collected from an online interactive free database of the Global Energy Observatory (GEO). Location and coordinate information was also collected from the GEO database. Although GEO ensures that high quality data and information are collected and made available, this database includes user-generated content and therefore the information requires validation from other reliable sources. The data collected from both sources, GEO and (13), were cross-validated against information provided by several governments, energy companies and independent international agencies. These include the Electricity Supply Corporation of Malawi, the Tanzania Electric Supply Company Limited, the Kenya Electricity Generating Company Limited, the Uganda Electricity Generation Company, Lesotho Highlands Development Authority, Bujagali Energy Limited (Uganda), power-technology.com (covering the global energy industry), HydroWorld.com (provides latest hydropower news), and the World Energy Council (a network of leaders and practitioners for delivering sustainable energy systems) (see Supplementary Table 14).

For proposed hydropower sites in eastern and southern Africa, information was also mainly compiled from (13) (Supplementary Table 14). The information available in (13) is based on several reports and studies. For the Zambezi basin, the Zambezi Basin Multi-Sector Investment Opportunity Analysis (MSIOA) (2010, Supplementary Table 14) and De Condappa and Barron (2013, Supplementary Table 14) for the Congo Basin were used. For the Nile Basin, the Ethiopian Power System Expansion Master Plan Study (EEPSCO, 2013, Supplementary Table 14), the East African Power Pool master plan (EAPP/EAC, 2011, Supplementary Table 14) and a number of feasibility and pre-feasibility study reports on hydropower development in Ethiopia and Tanzania, (Ministry of Water Resources – Ethiopia, 2010; Ministry of Energy and Minerals – Tanzania, 2013 were used, Supplementary Table 14). For the Nile Basin (13) augmented the information through consultations with senior officials from the Nile Basin Initiative member countries.

Coordinates of proposed sites were determined manually based on descriptions given in project proposal documents and reports available freely online. These included information available on the Ministry and electricity generation company websites (Ministry of Water and Energy – Ethiopia, Zambezi River Authority 2015, Uganda Electricity Generation Company, Supplementary Table 14), a hydropower potential report (State of the River Nile Basin 2012, Supplementary Table 14), and hydropower, energy and power related news articles (HydroWorld.com and International Hydropower Association, Supplementary Table 14). An example of information available is the proposed site for the Tams Dam in Ethiopia, 45km from the town of Gambella. Here, a location on the river Baro at the specified distance of 45km was mapped on Google Earth to obtain the necessary coordinates for the proposed Tams Dam.

Supplementary References

- (1) Harris I, Jones P D, Osborn T J, Lister D H. Updated high-resolution grids of monthly climatic observations - the CRU TS3.10 Dataset. *Int J of Climatol.* **34**, 623-642. (2014) doi: 10.1002/joc.3711.
- (2) Gillett, N. P., T. D. Kell, P. D. Jones. Regional climate impacts of the Southern Annular Mode. *Geophys. Res. Lett.*, **33** L23704, doi:10.1029/2006GL027721. (2006)
- (3) Marchant, R., Mumbi, C., Behera, S., Yamagata, T. The Indian Ocean dipole – the unsung driver of climatic variability in East Africa. *African Journal of Ecology* **45** 4–16 (2007).
- (4) Owiti Z., Ogallo L.A. and Mutemi J. Linkages between the Indian Ocean Dipole and East African seasonal rainfall anomalies. *J. Kenya Meteorol. Soc.* **2** 3-17 (2008).
- (5) Conway, D., Hanson, C.E., Doherty, R., Persechino, A. GCM simulations of the Indian Ocean dipole influence on East African rainfall: Present and future. *Geophys. Res. Lett.*, **34**, L03705 (2007).
- (6) Nicholson, S. E. A review of climate dynamics and climate variability in Eastern Africa. In, Odada, E.O. et al. *The limnology, climatology and paleoclimatology of the East African lakes*, pp. 25-56. (1996).
- (7) Osborn TJ, Barichivich J, Harris I, van der Schrier G, Jones PD (2016) Monitoring global drought using the self-calibrating Palmer Drought Severity Index [in "State of the Climate in 2015"]. *Bulletin of the American Meteorological Society* **97**, S32-S36.
- (8) Block, P., Rajagopalan, B. (2007) Interannual variability and ensemble forecast of Upper Blue Nile Basin Kiremt season precipitation. *Journal of Hydrometeorology*, **8**(3), 327-343.
- (9) Eltahir, E. A. El Niño and the natural variability in the flow of the Nile River. *Water Resources Research* **32**, 131-137 (1996)
- (10) Becker, A., Finger, P., Meyer-Christoffer, A., Rudolf, B., Schamm, K., Schneider, U., and Ziese, M. A description of the global land-surface precipitation data products of the Global Precipitation Climatology Centre with sample applications including centennial (trend) analysis from 1901–present. *Earth System Science Data* **5**, 71-99 (2013).
- (11) Conway, D. Persechino, A., Ardoin-Bardin, S., Hamandawana, H., Dieulin, C., Mahe, G. Precipitation and water resources variability in sub-Saharan Africa during the 20th century. *J of Hydromet.* **10**, 41-59 (2009).
- (12) Maidment, R.I., Allan, R.P. and Black, E. Recent observed and simulated changes in precipitation over Africa. *Geophysical Research Letters*, **42**(19), 8155-8164 (2015).
- (13) Cervigni, R., Liden, M. J. R. Neumann, J. L. Strzepak, K. M. 2015. Enhancing the climate resilience of Africa's infrastructure : the power and water sectors. Africa Development Forum. Washington, D.C. World Bank Group.